Discontinuous Galerkin Method for Solving Magnetohydrodynamic Equations

A. Das Gupta and S. Roy
Applied Physics Research Group, University of Florida, Gainesville, FL, 32611

This abstract discusses the implementation of viscous compressible magnetohydrodynamic (MHD) equations using Discontinuous Galerkin method. Both one-dimensional and two dimensional MHD equations are solved and validation results are presented. The code uses a local Lax-Friedrichs flux for the inviscid numerical fluxes and BR2 scheme for the viscous fluxes. An eight wave formulation [1] is implemented to reduce the divergence errors in the two dimensional simulations. The in house code predicts results accurately when compared to the published results.

Nomenclature

ρ	=	density
$\mathbf{B}$	=	magnetic field vector
B_x	=	X component of magnetic field
B_y	=	Y component of magnetic field
E	=	total specific internal energy
$\mathbf{v}$	=	velocity vector
S_v	=	Viscous Lundquist number
S_r	=	Resistive Lundquist number
$\overline{\overline{\tau}}$	=	shear stress tensor

I. Introduction

Discontinuous Galerkin (DG) method has been found to be a robust numerical algorithm to solve for a variety of problems. The greatest advantage of this method is its parallelizability and the capability to handle complex geometries and discontinuities or strong gradients without producing spurious oscillations. It has been used to solve convection dominated problems, elliptic problems and convection-diffusion problems. The interest in solving MHD equations arises from the fact that it has lot of industrial and astronomical applications such as magnetic pump, magnetic damping and stirring during casting, plasma confinement, solar wind, plasma thrusters, motion in earth's core etc. In this paper we use modal Discontinuous Galerkin method for solving MHD equations. This method was originally introduced by Reed and Hill [2] for solving neutron transport equation. Extensive research was done on solving hyperbolic equations like Euler equations of gas dynamics, ideal MHD equations. Then it was extended to solve convection diffusion problems, using the so called Local Discontinuous Galerkin (LDG) [3] method. However due to the method's (LDG) large memory requirement we have used BR2 [4] scheme which is a compact form of the LDG method. This method has been proven to be both stable and consistent. The challenge in solving 2D inviscid MHD equations is that it develops singularities in a finite time, even with periodic boundary conditions and smooth initial conditions. Pouquet [5] suggested that 2D MHD turbulence is dynamically very similar to 3D hydrodynamic turbulence. However she proved that the small scale structures in 2D MHD turbulence are excited at a much higher level than 2D hydrodynamic turbulence. These small scale structures of 2D MHD flow are more intermittent than the small scale structures of 2D hydrodynamic flow.

II. Discontinuous Galerkin Formulation

Discontinuous Galerkin method is a finite element method in which the solution is approximated by piecewise continuous functions within the element with no global continuity requirement. Thus the numerical solution is discontinuous across the element interfaces. We have used Legendre polynomials for our 1D and Jacobi polynomials for our 2D simulations as our basis functions.

We present here the generic system of convection diffusion equations to show the discretization method.

$$\frac{\partial \vec{U}}{\partial t} + \nabla \cdot \mathbf{F}^i\left(\vec{U}\right) = \mu \nabla \cdot \mathbf{F}^v\left(\vec{U}, \nabla \vec{U}\right) \tag{1}$$

Where **U** denotes the vector of conserved variables, $\mathbf{F}^i$ and $\mathbf{F}^v$ denote the inviscid flux and viscous flux respectively. We shall present the formulation for the inviscid and viscous part of the equations separately. Before we move on to our formulation we shall briefly discuss the modal basis functions used in our formulation.

A. Modal Basis Functions

For our 1D simulation we use the Jacobi polynomials given by

$$P_n^{0,0}(x) = \frac{1}{2^n n!}\frac{d^n}{dx^n}[(x^2-1)^n]$$

This form of Jacobi polynomials is also called the Legendre polynomials. Our basis functions are given by

$$\varphi_p(\xi) = P_p^{0,0}(\xi)$$

Where ξ is the transformed coordinate system in [0, 1]. For 2D simulation we use the basis functions provided in the table below

Table 1. 2D Basis Functions

Basis/Order	1	2	3
1	1	1	1
2		$-1+2\,\xi$	$-1+2\,\xi$
3		$-1+2\,\eta$	$-1+2\,\eta$
4			$1-6\,\xi+6\xi^2$
5			$1-2\,\xi-2\,\eta+4\xi\eta$
6			$1-6\,\eta-6\eta^2$

Where ξ and η are the transformed coordinate system in [0, 1] × [0, 1]

B. Inviscid Formulation

To explain the formulation we take the inviscid part of Eq. (1). This is given by

$$\frac{\partial \vec{U}}{\partial t} + \nabla \cdot \mathbf{F}^i\left(\vec{U}\right) = 0 \tag{2}$$

We start with the variation statement of the standard Galerkin formulation by multiplying a test function to Eq. (2) and integrating by parts.

$$\int_{\Omega} v \frac{\partial \vec{U}}{\partial t} d\Omega - \int_{\Omega} \nabla v \cdot \mathbf{F}^i\left(\vec{U}\right) d\Omega + \int_{\Gamma} v \hat{n} \cdot \mathbf{F}^i\left(\vec{U}\right) d\sigma = 0 \tag{3}$$

To construct a DG discretization of Eq. (3) we consider an approximation Ω_h of Ω and a triangulation of T_h of Ω_h. We replace the exact solution U by U_h and the test space by V_h. Let the neighboring element be 'a'. Then Eq. (3) for the element 'k' is as follows

$$\int_{\Omega_{h,k}} v_h \frac{\partial \vec{U}_h}{\partial t} d\Omega - \int_{\Omega_{h,k}} \nabla v_h \cdot \mathbf{F}^i\left(\vec{U}_h\right) d\Omega + \sum_{e \in \partial\Omega_{h,k}} \int_e v_h \hat{\mathbf{F}}^i\left(\vec{U}_h, \vec{U}_h^a, \hat{n}\right) d\sigma = 0 \tag{4}$$

Summations in the above equation are mandatory because the integration by parts cannot be applied to an entire domain having discontinuities at element interfaces. In the above formulation the flux function $\hat{\mathbf{F}}^i$ is the numerical flux. In our present work we have chosen the Local Lax-Friedrichs flux which is a consistent two point monotone Lipschitz flux and α is an estimate of the biggest eigenvalue of the jacobian $\left(\partial F/\partial U\right) \cdot n$.

$$\hat{\mathbf{F}}^i(\vec{U}_h, \vec{U}_h^a, \hat{n}) = \frac{1}{2}\left[\mathbf{F}^i(\vec{U}_h) \cdot \hat{n} + \mathbf{F}^i(\vec{U}_h^a) \cdot \hat{n} - \alpha(\vec{U}_h^a - \vec{U}_h)\right]$$

C. Viscous Formulation

The viscous part of the Eq. (1) is formulated using the BR2 [4] scheme to avoid using auxiliary variables as used in Local Discontinuous Galerkin method. The equation system is first reduced to first order by creating an auxiliary equation.

$$\nabla \vec{U} - \vec{\theta} = 0 \tag{5}$$

$$\frac{\partial \vec{U}}{\partial t} + \nabla \cdot \mathbf{F}^i\left(\vec{U}\right) = \mu \nabla \cdot \mathbf{F}^v\left(\vec{U}, \vec{\theta}\right) \tag{6}$$

Discretization of the above equation will give us

$$\int_{\Omega} \tau \vec{\theta} d\Omega - \int_{\Omega} \nabla \tau \cdot \vec{U} d\Omega - \int_{\Gamma} \tau \vec{U} \cdot \hat{n} d\sigma \tag{7}$$

$$\int_{\Omega} v \frac{\partial \vec{U}}{\partial t} d\Omega - \int_{\Omega} \nabla v \cdot \mathbf{F}^i\left(\vec{U}\right) d\Omega + \int_{\Gamma} v \hat{n} \cdot \mathbf{F}^i\left(\vec{U}\right) d\sigma + \int_{\Omega} \nabla v \cdot \mathbf{F}^v\left(\vec{U}, \vec{\theta}\right) d\Omega - \int_{\Gamma} v \hat{n} \cdot \mathbf{F}^v\left(\vec{U}, \vec{\theta}\right) d\sigma = 0 \tag{8}$$

The first half of Eq. (8) is the inviscid formulation so we shall discuss the second half of Eq. (8) and Eq. (7) for our viscous formulation. Taking the same basis function for Eq. (7) and Eq. (8) and using the same approximations as the inviscid part we have

$$\int_{\Omega_{h,k}} v_h \vec{\theta}_h d\Omega - \int_{\Omega_{h,k}} \nabla v_h \cdot \vec{U}_h d\Omega - \int_e v_h \hat{\mathbf{H}}_{aux}\left(\vec{U}_h, \vec{U}_h^a\right) \cdot \hat{n} d\sigma \tag{9}$$

$$Inviscid + \int_{\Omega_{h,k}} \nabla v_h \cdot \mathbf{F}^v\left(\vec{U}_h, \vec{\theta}_h\right) d\Omega - \sum_{e \in \partial\Omega_{h,k}} \int_{\Gamma} v_h \hat{n} \cdot \hat{\mathbf{H}}^v_{aux}\left(\vec{U}_h, \vec{U}_h^a, \vec{\theta}_h, \vec{\theta}_h^a\right) d\sigma = 0 \tag{10}$$

If BR1 is used then the flux denoted by $\hat{\mathbf{H}}_{aux}$ and $\hat{\mathbf{H}}^v_{aux}$ will be given by

$$\widehat{\mathbf{H}}_{aux} = \frac{1}{2}\left(\vec{U}_h + \vec{U}_h^a\right)$$

$$\widehat{\mathbf{H}}_{aux}^v = \frac{1}{2}\left[\mathbf{F}^v\left(\vec{U}_h, \vec{\theta}_h\right) + \mathbf{F}^v\left(\vec{U}_h^a, \vec{\theta}_h^a\right)\right]$$

We can see that for Eq. (10) if the auxiliary variable is evaluated before solving, then Eq. (9) can be removed from the system of equations. Thus the matrix to be solved would be much smaller. To do this BR2 [6] method is employed and using lift operators we evaluate θ in the domain, at the element interfaces and boundary edges. Once θ is evaluated we use the same flux as used in BR1 method just replacing θ with the value obtained.

III. Governing Equations for viscous MHD equations

The nondimensional equations for compressible magnetohydrodynamics can be expressed in conservative form as

$$\frac{\partial \rho}{\partial t} + \nabla \cdot (\rho \mathbf{v}) = 0 \tag{11}$$

$$\frac{\partial (\rho \mathbf{v})}{\partial t} + \nabla \cdot \left(\rho \mathbf{v}\mathbf{v}^t - \mathbf{B}\mathbf{B}^t + \left(p + \frac{1}{2}|\mathbf{B}|^2 \right)\mathbf{I} - \frac{1}{S_v}\overline{\overline{\tau}} \right) = 0 \tag{12}$$

$$\frac{\partial \mathbf{B}}{\partial t} + \nabla \times \left(\mathbf{B} \times \mathbf{v} + \frac{1}{S_r}\nabla \times \mathbf{B} \right) = 0 \tag{13}$$

$$\frac{\partial E}{\partial t} + \nabla \cdot \left((E + p)\mathbf{v} + \left(\frac{1}{2}|\mathbf{B}|^2 \mathbf{I} - \mathbf{B}\mathbf{B}^{\mathrm{T}} \right) \cdot \mathbf{v} - \frac{1}{S_v}\mathbf{v} \cdot \overline{\overline{\tau}} + \frac{1}{S_r}\left[\mathbf{B} \cdot \nabla \mathbf{B} - \nabla \left\{ \frac{1}{2}|\mathbf{B}|^2 \right\} \right] - \frac{1}{S_v \,\mathrm{Pr}} \nabla \mathrm{T} \right) = 0 \tag{14}$$

$$\nabla \cdot \mathbf{B} = 0 \tag{15}$$

Where, S_v and S_r are the viscous Lundquist number and Resistive Lundquist numbers and the total pressure p, is given by $p = (\gamma - 1)\left(\rho E - \frac{1}{2}\rho |\mathbf{v}|^2 - \frac{1}{2}|\mathbf{B}|^2 \right)$

The last equation called the divergence free condition comes from the fact that there can be no magnetic monopoles. To deal with this equation different constraint transport methods are used. In our work we have used the approach presented by Powell [1]. The equation system is changed so that the Jacobian matrix includes an "eighth-wave" which is the divergent mode that corresponds to the velocity u. The modification to the equation compromises the conservative formulation of the scheme but the deviations are very small. Thus the equation system becomes

$$\frac{\partial \rho}{\partial t} + \nabla \cdot (\rho \mathbf{v}) = 0 \tag{16}$$

$$\frac{\partial (\rho \mathbf{v})}{\partial t} + \nabla \cdot \left(\rho \mathbf{v}\mathbf{v}^t - \mathbf{B}\mathbf{B}^t + \left(p + \frac{1}{2}|\mathbf{B}|^2 \right)\mathbf{I} - \frac{1}{S_v}\overline{\overline{\tau}} \right) = -\mathbf{B}\nabla \cdot \mathbf{B} \tag{17}$$

$$\frac{\partial \mathbf{B}}{\partial t} + \nabla \times \left(\mathbf{B} \times \mathbf{v} + \frac{1}{S_r}\nabla \times \mathbf{B} \right) = \mathbf{v}\nabla \cdot \mathbf{B} \tag{18}$$

$$\frac{\partial E}{\partial t} + \nabla \cdot \left((E + p)\mathbf{v} + \left(\frac{1}{2}|\mathbf{B}|^2 \mathbf{I} - \mathbf{B}\mathbf{B}^{\mathbf{t}} \right) \cdot \mathbf{v} - \frac{1}{S_v}\mathbf{v} \cdot \overline{\overline{\tau}} + \frac{1}{S_r}\left[\mathbf{B} \cdot \nabla \mathbf{B} - \nabla \left\{ \frac{1}{2}|\mathbf{B}|^2 \right\} \right] - \frac{1}{S_v \,\mathrm{Pr}} \nabla \mathrm{T} \right) = (\mathbf{v} \cdot \mathbf{B})\nabla \cdot \mathbf{B} \tag{19}$$

A. 1D MHD Results

To validate our code we solve the case presented by Brio and Wu [5]. For the 1D simulation Eq. (11) through Eq. (14) are used without the viscous terms. The initial data used are identical to Sod's Shock tube problem. The initial conditions, $\rho_l = 1,\ u_l = 0,\ v_l = 0,\ p_l = 1,\ B_{y,l} = 1$ and $\rho_r = 0.125,\ u_r = 0,\ v_r = 0,\ p_r = 0.1,\ B_{y,r} = -1$ are for the left and right states of the shock tube. To satisfy the divergence free condition $B_x = 0.75$ is chosen and $\gamma = 2$ is used. The results shown in figure 1 are matching with the results given by Brio and Wu.

It has been proven that the nonconvex [6] nature of MHD equations results in complicated wave structures like, compound waves consisting of a shock and attached to it a rarefaction wave of the same family. From the figures shown above we can see a fast rarefaction wave, slow compound wave, a contact discontinuity, a shock and a right moving rarefaction wave.

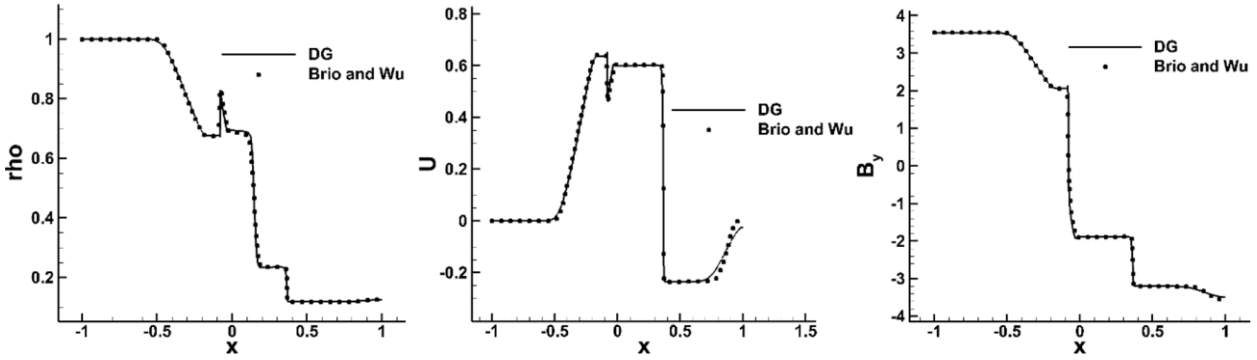

FIG. 1. Validation case for 1D MHD equations with Brio and Wu solution

B. 2D MHD Results

In MHD flow the relative movement of the conducting fluid and the imposed magnetic field causes an e.m.f. to develop in accordance with the Faraday's law of induction. Thus current will be induced which in turn will give rise to induced magnetic field. This adds to the imposed magnetic field and the change causes the fluid to be dragged [7] by the magnetic field lines along with it. Thus the combined (imposed and induced) magnetic field gives rise to Lorentz force when they interact with the induced current density and inhibit the relative movement of fluid and magnetic field. However when these lines of forces snap due to stretching they interact with the flow and produce small eddies on top of larger convecting ones. However the explanation of the entire process of MHD turbulence is lot more complicated to be discussed here completely.

1. Ideal MHD results

To test the 2D MHD code the inviscid part of Eq. (15) through Eq. (18) are solved. We have chosen the compressible form of Orszag Tang vortex problem [8] which was presented by Dahlburg and Picone [9]. This is one of the widely used cases for validation of the 2D MHD code. The initial conditions are non-random, periodic with the velocity fields and magnetic field being divergence free. The domain size is [1×1] and three different meshes have been used to obtain the results. In Fig. 3 the upper left image is for 64×64 mesh, upper right for 128×128 mesh and lower left for 256×256 mesh. The initial conditions for this problem are given by

$$\rho = \frac{25}{36\pi};\ p = \frac{5}{12\pi};\ u = -\sin(2\pi y);\ v = \sin(2\pi x);\ B_x = -\frac{1}{\sqrt{4\pi}}\sin(2\pi y);$$

$$B_y = \frac{1}{\sqrt{4\pi}}\sin(4\pi x)$$

The boundary conditions are periodic everywhere. The results shown in Fig. 4 are compared with the solution obtained from the Athena code. The pressure at the location y = 0.4277 has been plotted in Fig. 3 and compared with the solution given by Athena MHD code and Londrillo & Del Zanna [10].

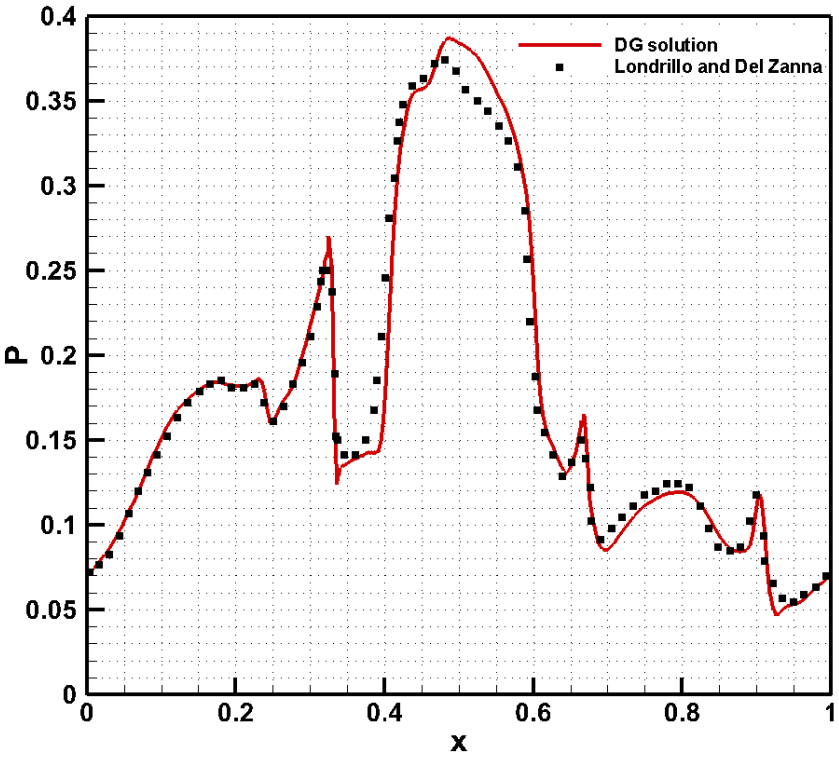

FIG. 2. Pressure contours at y = 0.4277

It was found by Dahlburg and Picone [9] as well as Orszag [8] that two dimensional MHD turbulence has excited small scale structures which are much stronger than the two dimensional hydrodynamic turbulence. The compressible form of the MHD equation gives rise to additional small scale structures such as massive jets and bifurcation of eddies. Our code captures these fine features and although there are some oscillations at the shocks the solution does not diverge. The simulation is started with average Mach number of M = 1.0, the density is chosen such that the initial speed of sound $c_s = 1$ for $\gamma = 5/3$. The maximum and minimum Mach numbers are 0 and 2 respectively.

2. Viscous MHD results

To understand the viscous effects and the compressibility effects of MHD equations Eq. (15) through Eq. (18) are solved. The solutions presented are compared with Dahlburg and Picone [9] assuming their same initial conditions and boundary conditions. Both S_v and S_r are taken as 100. The contours shown in figure 4 and figure 5 are streamlines for velocity field and magnetic field respectively. We can clearly see that the results match with the published results accurately. The code did not require the use of slope limiters to solve the governing equations. Figure 4 clearly depicts the considerable difference in velocity field. Dahlburg and Picone [9] attributed this to the increased rate of reconnection caused by the compressibility effects.

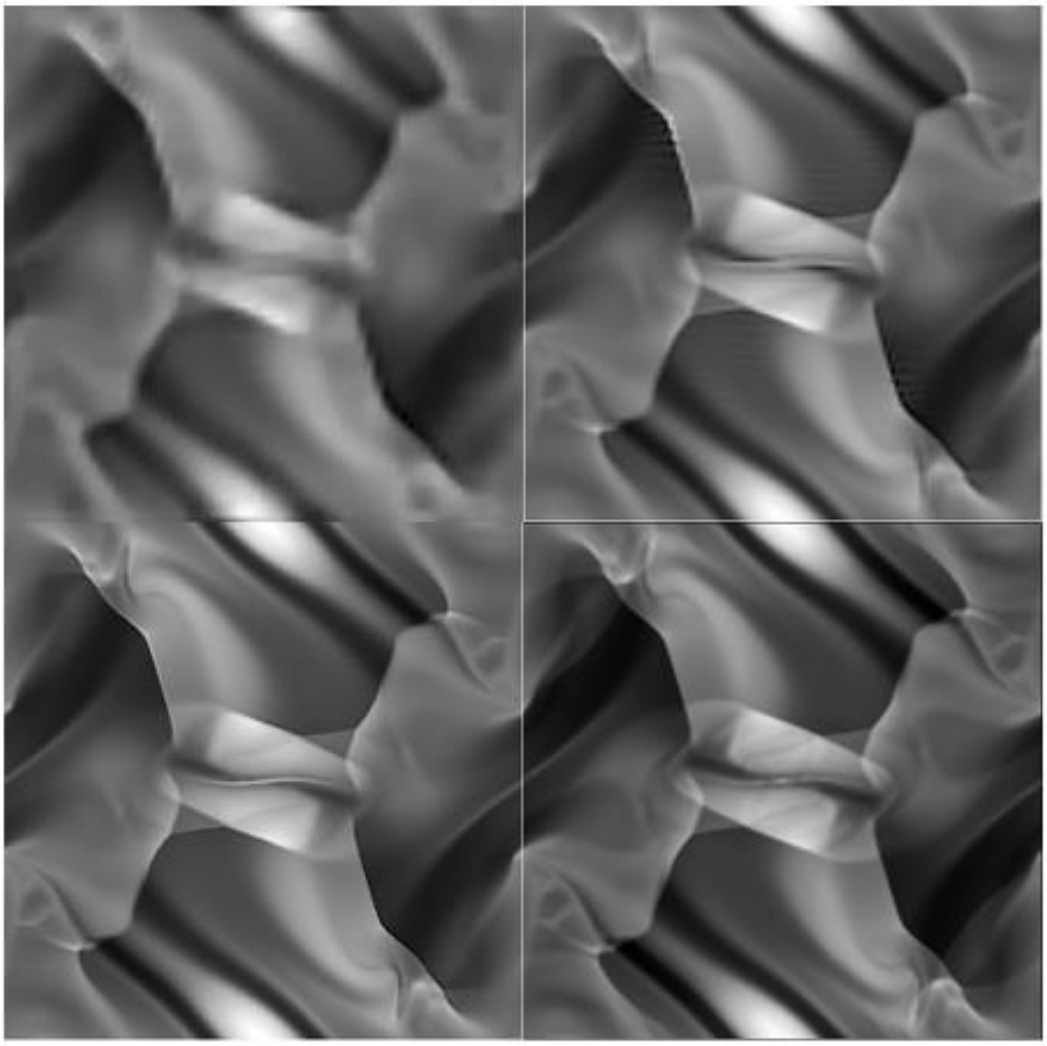

FIG. 3. Compressible Orszag Tang Vortex at t = 0.5 Top left, solution with 64x64 elements, Top right, solution with 128x128 elements, Bottom left, solution with 256x256 elements, Bottom right, solution obtained using Athena code for 192x192 elements.

However, the magnetic streamlines depicted in figure 5 do not show significant changes due to compressibility. To see the effects of compressibility we look at the magnetic streamlines at a later time and still find an insignificant amount of variation as seen in figure 6.

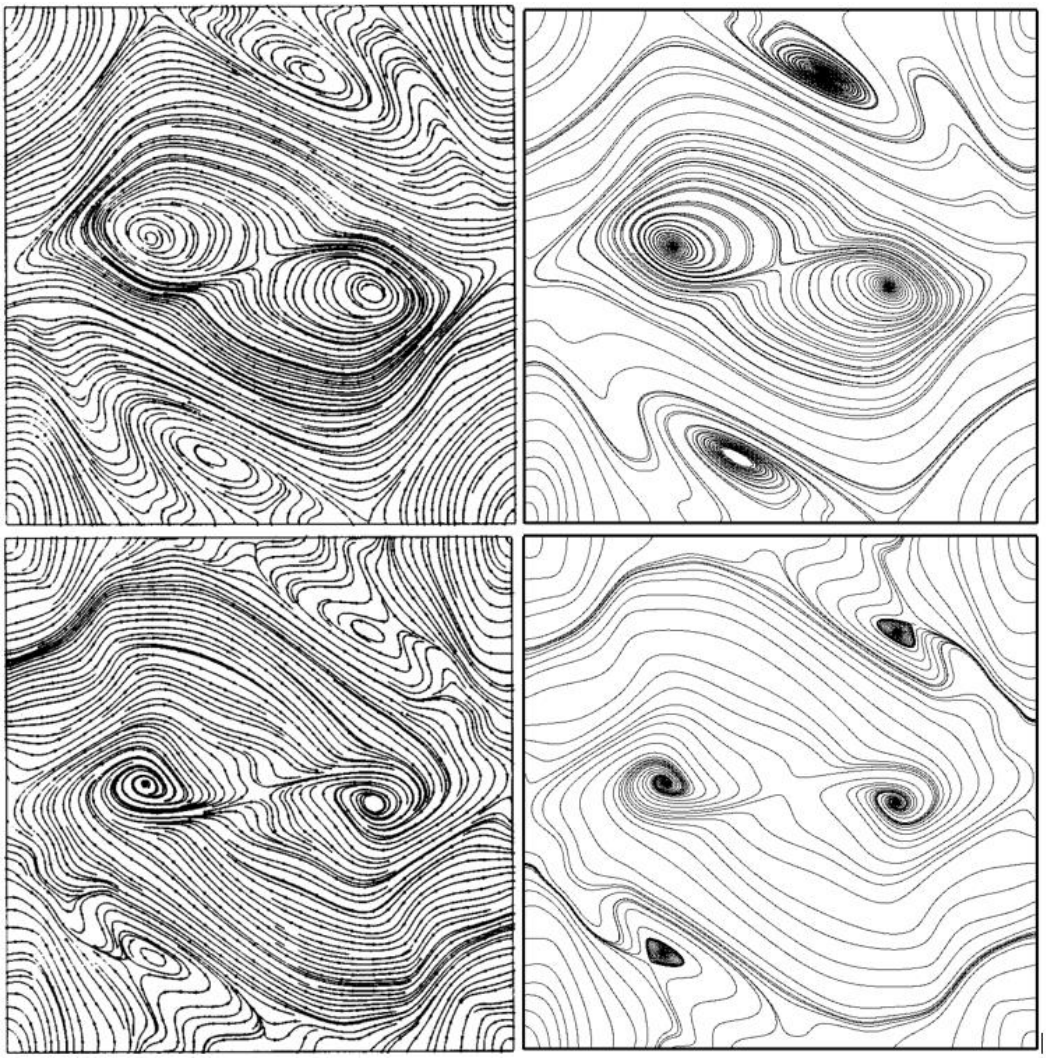

FIG. 4. Velocity Streamlines for Orszag Tang vortex at time = 0.2, left column are published results [9] and the right column are the solutions obtained. (Top) M = 0.2 and (bottom) M = 0.6

IV. Summary

The validation results for MHD flow have been presented and our in house code shows accurate results when compared to literature. Discontinuous Galerkin method doesn't require any slope limiter or shock capturing method to solve the problems presented in this paper. The use of BR2 scheme for the viscous fluxes have proven beneficial in saving computational time and making the system more stable and consistent. Although 2D MHD equations have used Powell [1] eight wave formulation, the effects of divergence error was not significant to alter the solutions. Also looking at the viscous non ideal MHD equations we see that the change in magnetic field is insignificant compared to the change in velocity field due to compressibility effects.

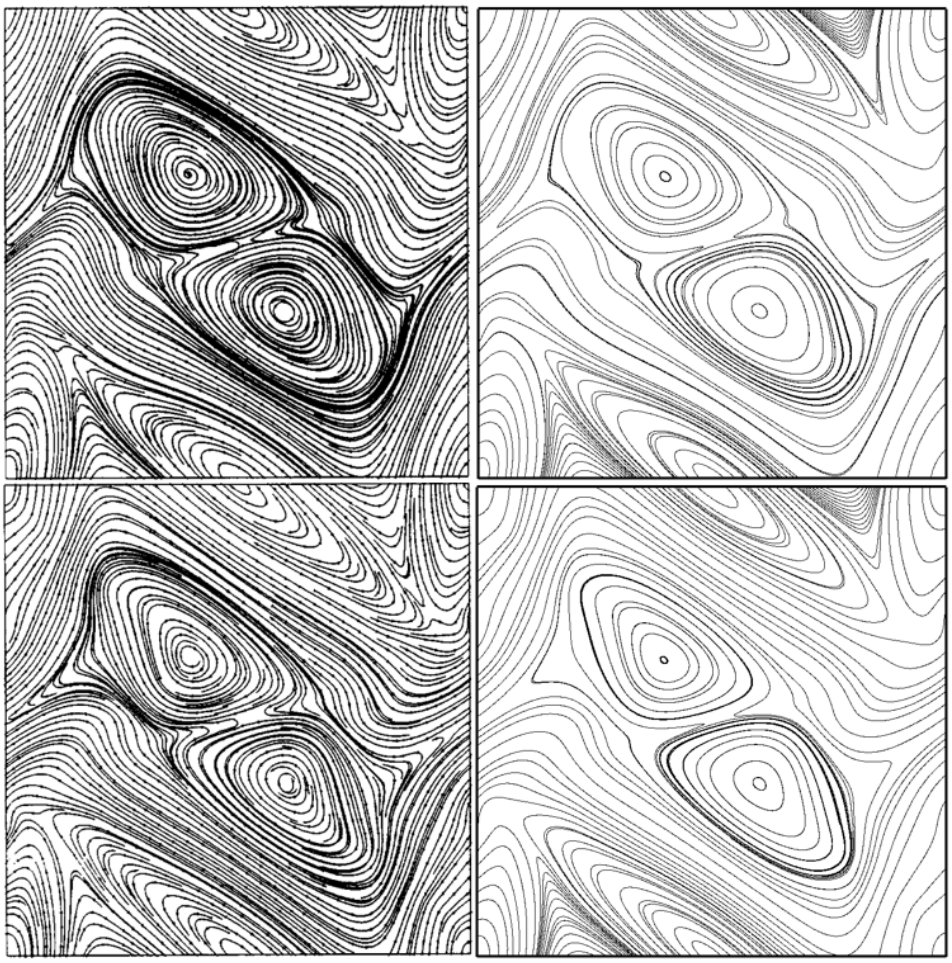

FIG. 5. Magnetic Streamlines for Orszag Tang vortex at time = 0.2, left column are published results [9] and the right column are the solutions obtained. (Top) left image is for incompressible and right for M = 0.2 and (bottom) M = 0.6

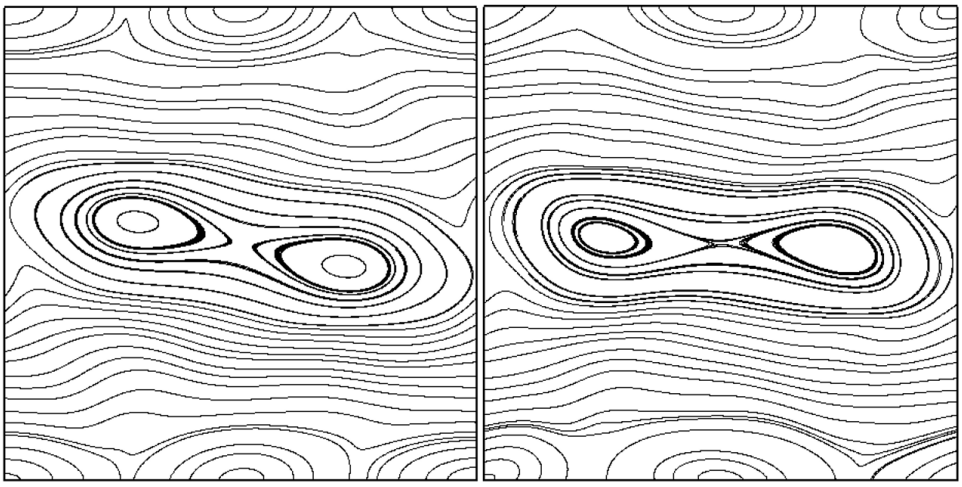

FIG. 6. Magnetic streamlines at time = 8. (Left) M = 0.2 and (right) M = 0.6

References

[1]Powell, K. G., "An Approximate Riemann Solver for Magnetohydrodynamics (that works in more than one dimension)," Technical report ICASE Report 94-24, ICASE, NASA Langley 1994.

[2]Reed, W.H. and Hill, T.R., "Triangular mesh methods for the neutron transport equation," Technical Report LA-UR-73-479, Los Alamos Scientific Laboratory, 1973

[3]Cockburn, B., and Shu, C.W., "The local discontinuous Galerkin method for time-dependent convection-diffusion systems," *SIAM Journal on Numerical Analysis*, 35, no. 6 (1998): 2440-2463.

[4]Bassi, F. and Rebay, S., "Discontinuous Galerkin solution of the Reynolds-averaged Navier-Stokes and k-ω turbulence model equations," *Journal of Computers & Fluids*, 34:507-540, 2005.

[5]Brio, M. and Wu, C.C., "An Upwind Differencing Scheme for Equations of Ideal Magnetohydrodynamics," *Journal of Computational Physics*, 75:400-422, 1988

[6]Pouquet, A., "On two-dimensional magnetohydrodynamic turbulence," *Journal of Fluid Mechanics*, 88, 1, 1978

[7]Davidson, P.A., "An Introduction to Magnetohydrodynamics", Cambridge University Press, 2001, Chap. 1

[8]Orszag, S A., and Tang, C., "Small Scale Structure of two-dimensional magnetohydrodynamic turbulence," *Journal of Fluid Mechanics*, 90:129-143, 1979

[9]Dahlburg, R. B., and Picone, J.M., "Evolution of Orszag Tang Vortex system in a compressible medium. I. Initial average Subsonic flow," *Physics of Fluids*, B 1(11), 2153, 1989

[10]Londrillo, P., and Del Zanna, L., "High-order upwind schemes for multidimensional magnetohydrodynamics," *The Astrophysical Journal*, 530(1), 508, 2000.